arXiv:2012.09962v5 [cs.LG] 27 Nov 2021

Addressing Feature Suppression in Unsupervised Visual Representations

Tianhong Li[1,*] Lijie Fan[1,*] Yuan Yuan[1] Hao He[1] Yonglong Tian[1]
Rogerio Feris[2] Piotr Indyk[1] Dina Katabi[1]

[1]MIT CSAIL, [2]MIT-IBM Watson AI Lab

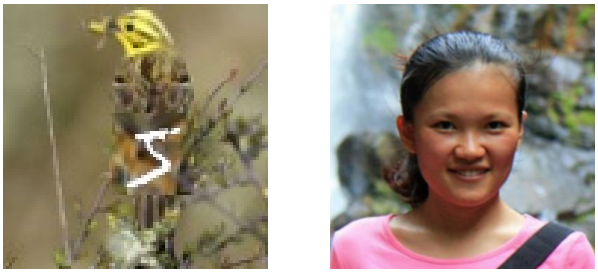
Abstract

Contrastive learning is one of the fastest growing research areas in machine learning due to its ability to learn useful representations without labeled data. However, contrastive learning is susceptible to feature suppression – i.e., it may discard important information relevant to the task of interest, and learn irrelevant features. Past work has addressed this limitation via handcrafted data augmentations that eliminate irrelevant information. This approach however does not work across all datasets and tasks. Further, data augmentations fail in addressing feature suppression in multi-attribute classification when one attribute can suppress features relevant to other attributes. In this paper, we analyze the objective function of contrastive learning and formally prove that it is vulnerable to feature suppression. We then present predictive contrastive learning (PCL), a framework for learning unsupervised representations that are robust to feature suppression. The key idea is to force the learned representation to predict the input, and hence prevent it from discarding important information. Extensive experiments verify that PCL is robust to feature suppression and outperforms state-of-the-art contrastive learning methods on a variety of datasets and tasks.

1. Introduction

The area of unsupervised or self-supervised representation learning is growing rapidly [2, 11, 13–15, 18, 21, 34, 36]. It refers to learning data representations that capture potential labels of interest, and doing so without human supervision. Contrastive learning is increasingly considered as a standard and highly competitive method for unsupervised representation learning. Features learned with this method have been shown to generalize well to downstream tasks, and in some cases surpass the performance of supervised models [3–5, 7, 23, 28].

Contrastive learning learns representations by contrasting positive samples against negative samples. During training, a data sample is chosen as an anchor (e.g., an image); positive samples are chosen as different augmented versions of the anchor (e.g., randomly cropping and color distorting the image), whereas negative samples come from other samples in the dataset.



(a) Digit & Bkgd (b) Face Attribute

Figure 1. (a) In Colorful-Moving-MNIST [27], the input has two types of information: digit and background object. But contrastive learning methods focus on the background object and ignore the digit. (b) Each image in FairFace [20] has multiple attributes such as age, gender, ethnicity, etc. Existing contrastive learning methods focus on ethnicity and partially ignore other attributes.

Yet contrastive learning is vulnerable to feature suppression – i.e., if simple features are contrastive enough to separate positive samples from negative samples, contrastive learning might learn such simple (or simpler) features even if irrelevant to the tasks of interest, and other more relevant features are suppressed. For example, the authors of [4] show that color distribution can be used to distinguish patches cropped from the same image, from patches from different images; yet such feature is not useful for object classification. Past work addresses this problem by designing handcrafted data augmentations that eliminate the irrelevant features, so that the network may learn the relevant information [4–7, 15].

However, in many scenarios it is hard to design augmentations to solve the problem of feature suppression. For example, the authors of [27] highlight the scenario in Figure 1 (a), where each image shows a digit (from MNIST) on a randomly chosen background object (from STL-10). They show that features related to background objects can create

*Indicates equal contribution.

a shortcut that prevent contrastive learning from learning features related to digits. In this case, one cannot simply eliminate the background information since such a design, though would help digit classification, would harm the background classification task. A similar problem exists in the task of human face attribute classification, where each face image can be used in multiple downstream tasks including gender, age, and ethnicity classification (Figure 1 (b)), but the features learned by contrastive learning can be biased to only one of the attributes (e.g., ethnicity) and show poor performance on other attributes (gender and age) as shown in the experiments section. It is hard to come up with data augmentations that eliminate the dominant attribute without harming the corresponding classification task. Moreover, as machine learning keeps expanding to new modalities it becomes increasingly difficult to design handcrafted data augmentations because many new modalities are hard to directly interpret by humans (e.g., acceleration from wearable devices), or the interpretation requires domain experts (e.g., medical data).

In this paper, we first provide a theoretical analysis of contrastive learning and prove it is vulnerable to feature suppression. Our analysis shows that even with large feature dimensions, contrastive learning has many local minimums that discard significant information about the input, and hence cause feature suppression. Furthermore, the value of the loss function at such local minimums is very close to its value at the global minimum, making it hard to propel the model out of such local minimums.

Second, we propose predictive contrastive learning (PCL) as a training scheme that prevents feature suppression. PCL learns representations using contrastive and predictive learning simultaneously. We use the term predictive learning to refer to tasks that force the representation to predict the input, such as inpainting, colorization, or autoencoding. Such tasks counter the effect of feature suppression because they force the learned features to retain the information in the input. More formally, if the contrastive loss (i.e., the InfoNCE loss) gets stuck in a local minimum that loses semantic information, the predictive loss naturally becomes very high, forcing the model to exit such local minimums. An interesting feature of PCL is that the predictive task is used only during training, and hence introduces no computation overhead during testing.

We evaluate PCL and compare it with state-of-the-art contrastive learning baselines on four different datasets: ImageNet, MPII [1], Colorful-Moving-MNIST [27], and FairFace [20]. For all tasks, PCL achieves superior performance and outperforms the state-of-the-art baselines by large margins, demonstrating robustness against feature suppression.

The paper makes the following contributions:

- It provides a theoretical analysis of contrastive learning that proves its vulnerability to feature suppression.
- It introduces PCL, an unsupervised learning framework that automatically avoids feature suppression and provides a representation that learns all of the semantics in the input and can support different downstream tasks and multi-attribute classification.
- It empirically shows that SOTA contrastive learning baselines (e.g., SimCLR, MoCo, and BYOL) suffer from feature suppression, and that PCL outperforms those baselines on several important tasks including object recognition, pose estimation, and face attribute classification.

2. Related Work

Early work on unsupervised representation learning has focused on designing pretext tasks and training the network to predict their pseudo labels. Such tasks include solving jigsaw puzzles [22], restoring a missing patch in the input [24], or predicting image rotation [12]. However, pretext tasks have to be handcrafted, and the generality of their representations is typically limited [4].

Hence, researchers have recently focused on contrastive learning, which emerged as a competitive and systematic method for learning effective representations without human supervision. The learned features generalize well to downstream tasks, outperform representations learned through pretext tasks, and even surpass the performance of supervised models on some tasks [4, 5, 7, 15]. Multiple successful contrastive learning frameworks have been proposed, which typically differ in the way they sample negative pairs. To name a few, SimCLR [4] uses a large batch size, and samples negative pairs within each batch. The momentum-contrastive approach (MoCo) [15] leverages a moving-average encoder and a queue to generate negative samples on the fly during training. Contrastive-Multiview-Coding [26] maintains a memory-bank to store features and generate negative samples. Some recent methods, like BYOL, do not rely on negative pairs [8, 13]. Instead, they use two neural networks that learn from each other to boost performance.

Past work has also reported problems with contrastive learning. It can focus on irrelevant features such as color distribution, and suppress more relevant features [4]. Past work addressed this problem by using color-distortion as a data augmentation. Also, the authors of [27] noted that when the data includes multiple types of semantics, contrastive learning may learn one type of semantics and fail to learn effective features of the other semantics (as in Figure 1(b) where the background object information can suppress features related to digits). They proposed a solution that learns contrastive views suitable for the desired downstream task. While they share our goal of supporting different downstream tasks, their method requires supervision since they learn their contrastive views from labeled data. In contrast, our approach is completely unsupervised.

Another related work is contrastive-predictive-coding

(CPC) [16, 23]. CPC has some similarities with PCL in that it has a predictive task that aims to reconstruct missing information. However, CPC aims to reconstruct the features of a future frame, while PCL reconstructs the raw input data. As a result, the representation learned by CPC is not forced to contain necessary information to reconstruct the input, making it susceptible to feature suppression, just like other contrastive learning methods.

The family of auto-encoders provides a popular framework for unsupervised representation learning using a reconstructive loss [17, 25, 30]. It trains an encoder to generate low-dimensional latent codes that could reconstruct the entire high-dimensional inputs. There are many types of AEs, such as denoising auto-encoders [30], which corrupt the input and let the latent codes reconstruct it, and variational auto-encoders [25], which force the latent codes to follow a prior distribution. PCL can be viewed as a special variant of the denoising auto-encoder that forces the latent codes to have a 'contrastive' property regularized by a contrastive loss. As a result, the latent codes, are good not only for reconstructing the input, but also for downstream classification tasks.

Finally, several concurrent papers published on Arxiv also used a combination contrastive and reconstructive loss [10, 19]. However, none of them explore the potential of this combination to solve the feature suppression problem, or provides a theoretical analysis of feature suppression. This paper is the first to demonstrate that the combination of contrastive and predictive loss can be used to avoid feature suppression and learn general representations that support multiple downstream tasks.

3. Analysis of Feature Suppression

Before delving into formal proofs, we provide an informal description of our analysis as follows:

1. At low feature dimensions, naturally the global minimum of contrastive learning loses semantic information because with small feature dimensions, it is impossible to keep all information about the input.
2. We prove in Corollary 2 that the global minimums of the contrastive learning loss (i.e., infoNCE) at low dimensions are local minimums at higher dimensions. Thus, even if contrastive learning uses high dimension features, it will have many local minimums, and those minimums lose semantic information about the input, i.e., they experience feature suppression.
3. We further prove in Lemma 1 and Figure 2 that the value of infoNCE at such local minimums can be very close to its global minimum, making it hard to escape from such local minimums.
4. The above three points mean that, even at high dimensions, contrastive learning is likely to get stuck in a local minimum that exhibits feature suppression. Adding a predictive loss allows the model to exit such local minimum and avoid feature suppression. This is because suppressed features lose information about the input causing the predictive loss to become large, and push the model out from such local minimum and away from feature suppression.

3.1. Formal Proof.

Let $X = \{x_i\}_{i=1}^n$ be the set of the data points. We use λ_{ij} to indicate whether a data pair x_i and x_j is positive or negative. Specifically, $\lambda_{ij} = 1$ indicates a positive pair while $\lambda_{ij} = 0$ indicates a negative pair. Let $Z = \{z_i\}_{i=1}^n$, where $z_i = f(x_i) = (z_i^1, \cdots, z_i^d) \in \mathbb{S}^{d-1}$, denote the learned features on the hypersphere, generated by the neural network f. We consider the following empirical asymptotics of the infoNCE objective function introduced in [31].

Definition 1 (Empirical infoNCE asymptotics)**.**

$$\mathcal{E}_{\texttt{limNCE}}(Z; X, t, d) \triangleq$$
$$-\frac{1}{tn^2}\sum_{ij}\lambda_{ij} z_i^\top z_j + \frac{1}{n}\sum_i \log\left(\frac{1}{n}\sum_j e^{z_i^\top z_j/t}\right)$$

We are going to connect the landscape of empirical infoNCE asymptotics in the low dimension to that in the high dimension. We start by defining a *lifting operator* that maps a low dimensional vector to a higher dimension.

Definition 2 (Lifting operator)**.** *A lifting operator $\mathcal{T}_\sigma$ parameterized by an indexing function σ maps a d_1-dimensional vector to dimension d_2 ($d_2 > d_1$). Its parameter σ is a permutation of length d_2. Given a d_1-dimensional vector z, the lifting operator maps it to a d_2-dimensional vector $\tilde{z} = \mathcal{T}_\sigma(z)$ by the following rules: $\tilde{z}^t = z^{\sigma(t)}$ if $\sigma(t) \le d_1$, otherwise $\tilde{z}^t = 0$.*

With a slight abuse of the notation, we allow the lifting operator to map a *set* of low dimensional vectors to higher dimension, i.e. $\mathcal{T}_\sigma(\{z_i\}) = \{\mathcal{T}_\sigma(z_i)\}$. We further allow the lifting operator to map a function f of lower dimension to higher dimension, i.e., $\mathcal{T}_\sigma(f)(x) = \mathcal{T}_\sigma(f(x))$. Note that $\mathcal{T}_\sigma$ is a linear operator. We highlight several useful properties of $\mathcal{T}_\sigma$:

Lemma 1 (Value Invariance)**.** *The value of the empirical infoNCE asymptotics is invariant under the lifting operation. Formally, consider any lifting operator $\mathcal{T}_\sigma$ from the dimension d_1 to the dimension d_2. We have*

$$\mathcal{E}_{\texttt{limNCE}}(\mathcal{T}_\sigma(Z); X, t, d_2) = \mathcal{E}_{\texttt{limNCE}}(Z; X, t, d_1)$$

Proof. Following the definition of $\mathcal{T}_\sigma$, $\forall z_i, z_j$, $z_i^\top z_j = \mathcal{T}_\sigma(z_i)^\top \mathcal{T}_\sigma(z_j)$. Therefore, $\mathcal{E}_{\texttt{limNCE}}(\mathcal{T}_\sigma(Z); X, t, d_2) = \mathcal{E}_{\texttt{limNCE}}(Z; X, t, d_1)$. □

Lemma 2 (Gradient Equivariance)**.** *The gradient of the empirical infoNCE asymptotics is equivariant under the lifting operation. Formally, consider any lifting operator $\mathcal{T}_\sigma$ from the dimension d_1 to the dimension d_2. We have*

$$\nabla_{\tilde{z_k}} \mathcal{E}_{\texttt{limNCE}}(\mathcal{T}_\sigma(Z); X, t, d_2) = \mathcal{T}_\sigma\left(\nabla_{z_k} \mathcal{E}_{\texttt{limNCE}}(Z; X, t, d_1)\right)$$

Proof.

$$\begin{aligned}
&\nabla_{z_k} \mathcal{E}_{\texttt{limNCE}}(Z; X, t, d_1) \\
&\triangleq \nabla_{z_k}\Big(-\frac{1}{tn^2}\sum_{ij}\lambda_{ij} z_i^\top z_j + \frac{1}{n}\sum_i \log\left(\frac{1}{n}\sum_j e^{z_i^\top z_j/t}\right)\Big) \\
&= -\frac{1}{tn^2}\Big(\sum_{i\neq k}\lambda_{ki} z_i + \sum_{i\neq k}\lambda_{ik} z_i + 2\lambda_{kk} z_k\Big) \\
&+ \frac{1}{tn}\frac{2z_k e^{z_k^\top z_k/t} + \sum_{j\neq k} z_j e^{z_k^\top z_j/t}}{\sum_j e^{z_k^\top z_j/t}} + \frac{1}{tn}\sum_{i\neq k}\frac{z_i e^{z_i^\top z_k/t}}{\sum_j e^{z_i^\top z_j/t}} \\
&= -\frac{1}{tn^2}\Big(\sum_{i}\lambda_{ki} z_i + \sum_{i}\lambda_{ik} z_i\Big) \\
&+ \frac{1}{tn}\frac{z_k e^{z_k^\top z_k/t} + \sum_j z_j e^{z_k^\top z_j/t}}{\sum_j e^{z_k^\top z_j/t}} + \frac{1}{tn}\sum_{i\neq k}\frac{z_i e^{z_i^\top z_k/t}}{\sum_j e^{z_i^\top z_j/t}}.
\end{aligned}$$

Since $\mathcal{T}_\sigma$ is a linear operator,

$$\begin{aligned}
&\mathcal{T}_\sigma\left(\nabla_{z_k} \mathcal{E}_{\texttt{limNCE}}(Z; X, t, d_1)\right) \\
&= -\frac{1}{tn^2}\Big(\sum_{i}\lambda_{ki} \tilde{z_i} + \sum_{i}\lambda_{ik} \tilde{z_i}\Big) \\
&+ \frac{1}{tn}\frac{\tilde{z_k} e^{z_k^\top z_k/t} + \sum_j \tilde{z_j} e^{z_k^\top z_j/t}}{\sum_j e^{z_k^\top z_j/t}} + \frac{1}{tn}\sum_{i\neq k}\frac{\tilde{z_i} e^{z_i^\top z_k/t}}{\sum_j e^{z_i^\top z_j/t}} \\
&= -\frac{1}{tn^2}\Big(\sum_{i}\lambda_{ki} \tilde{z_i} + \sum_{i}\lambda_{ik} \tilde{z_i}\Big) \\
&+ \frac{1}{tn}\frac{\tilde{z_k} e^{\tilde{z_k}^\top \tilde{z_k}/t} + \sum_j \tilde{z_j} e^{\tilde{z_k}^\top \tilde{z_j}/t}}{\sum_j e^{\tilde{z_k}^\top \tilde{z_j}/t}} + \frac{1}{tn}\sum_{i\neq k}\frac{\tilde{z_i} e^{\tilde{z_i}^\top \tilde{z_k}/t}}{\sum_j e^{\tilde{z_i}^\top \tilde{z_j}/t}} \\
&= \nabla_{\tilde{z_k}} \mathcal{E}_{\texttt{limNCE}}(\mathcal{T}_\sigma(Z); X, t, d_2)
\end{aligned}$$

where $\tilde{z_k} = \mathcal{T}_\sigma(z_k)$. The second equality comes from the fact that $\forall z_i, z_j$, $z_i^\top z_j = \mathcal{T}_\sigma(z_i)^\top \mathcal{T}_\sigma(z_j)$. Thus $\nabla_{\tilde{z_k}} \mathcal{E}_{\texttt{limNCE}}(\mathcal{T}_\sigma(Z); X, t, d_2)$ equals $\mathcal{T}_\sigma\left(\nabla_{z_k} \mathcal{E}_{\texttt{limNCE}}(Z; X, t, d_1)\right)$, for all $z_k \in Z$. □

Corollary 1. *For any lifting operator $\mathcal{T}_\sigma$, if $\hat{Z} = \{\hat{z_i}\}$ is a stationary point of $\mathcal{E}_{\texttt{limNCE}}(Z; X, t, d_1)$, then $\mathcal{T}_\sigma(\hat{Z})$ is a stationary point of $\mathcal{E}_{\texttt{limNCE}}(Z; X, t, d_2)$.*

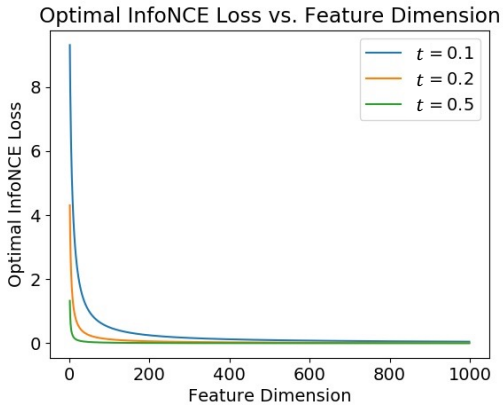


Figure 2. Optimal infoNCE loss vs. different output feature dimension d and temperature t.

Proof. The proof is in the supplemental material. □

Corollary 2. *For any lifting operator $\mathcal{T}_\sigma$, if $\hat{Z} = \{\hat{z_i}\}$ is a global minimum of $\mathcal{E}_{\texttt{limNCE}}(Z; X, t, d_1)$ with a positive definite Hessian matrix, then $\mathcal{T}_\sigma(\hat{Z})$ is a saddle point or a local minimum of $\mathcal{E}_{\texttt{limNCE}}(Z; X, t, d_2)$.*

Proof. The proof is in the supplemental material. □

With Corollary 4, we can explain why contrastive learning can suffer from feature suppression. Suppose f is a network that achieves the global minimum of $\mathcal{E}_{\texttt{limNCE}}(Z; X, t, d_1)$. When d_1 is relatively small (e.g., <100 for images), f must lose some information about the input, i.e., suppress feature. From Corollary 4, $\mathcal{T}_\sigma(f)$ is a saddle point or a local minimum of $\mathcal{E}_{\texttt{limNCE}}(Z; X, t, d_2)$ where $d_2 > d_1$ and $\mathcal{T}_\sigma(f)$ carries no more information than f. Therefore, for any dimension $d > 1$, there exists saddle point/local minimum of $\mathcal{E}_{\texttt{limNCE}}(Z; X, t, d)$ which suppresses features.

Furthermore, the value of the aforementioned saddle point/local minimum of $\mathcal{E}_{\texttt{limNCE}}(Z; X, t, d)$ is quite close to that of the global minimum. This is because the optimal value of $\mathcal{E}_{\texttt{limNCE}}(Z; X, t, d)$ converges quickly as d increases. Figure 2 shows the curve of $\log_0 F_1(; d; \frac{1}{4t^2})$, which is the optimal value of the infoNCE loss [32]. As shown in the figure, the curve essentially converges when $d > 200$. Therefore, $\mathcal{T}_\sigma(f)$ can be a saddle point/local minimum of $\mathcal{E}_{\texttt{limNCE}}(Z; X, t, d_2)$, and its value can also be quite close to that of the global minimum, making it hard to escape from such local minimum. So effectively one can achieve a value pretty close to the global minimum by suppressing features, and stay at that saddle point being unable to escape. This motivates our solution, which adds a predictive loss to force the model out from such local minimums that suppress features.

4. Predictive Contrastive Learning (PCL)

Predictive contrastive learning (PCL) is a framework for self-supervised representation learning. It aims to learn representations that are robust to feature suppression, and capable of supporting multiple diverse downstream tasks.

The idea underlying PCL is as follows: feature suppression is harmful because the representation loses important information that was available in the input. Thus, to counter feature suppression, PCL uses a prediction loss to ensure that the representation can restore the input, i.e., the features have the information available at the input. Yet, keeping all information in the features is not enough; the input already has all information. By adding a contrastive loss, PCL reorganizes the information in the feature space to make it amenable to downstream classification, i.e., samples that have similar attributes/objects are closer to each other than samples that have different attributes/objects. Figure 3 shows the PCL framework which has two branches: a contrastive branch and a predictive branch.

(a) Contrastive Branch: The contrastive branch is illustrated in the orange box in Figure 3. Here, we use SimCLR as an example to demonstrate the basic idea. However, this contrastive branch can be easily adapted to any contrastive learning method such as CPC, MoCo, and BYOL. For each image, we first generate a pair of positive samples by using two random augmentations τ_1 and τ_2, then we forward the two augmented inputs separately to the encoder E, parameterized by θ and a multi-layer nonlinear projection head H parameterized by h to get the latent representations z_1 and z_2 for these two positive samples. We use the commonly used InfoNCE loss [4] as the contrastive loss $\mathcal{L}_c$. Namely, for a batch of N different input images $x_i, i = 1, ..., N$,

$$\mathcal{L}_c = -\sum_{i=1}^{N} \log \sum \frac{\exp\left(\text{sim}(z_{2i}, z_{2i+1})/t\right)}{\sum_{k=1}^{2N} \mathbb{1}_{k\neq 2i} \exp\left(\text{sim}(z_{2i}, z_k)/t\right)},$$

where $\text{sim}(u, v) = u^T v/(\|u\|_2\|v\|_2)$ denotes the dot product between the normalized u and v (i.e., cosine similarity), $t \in \mathbb{R}^+$ is a scalar temperature parameter, and z_{2i}, z_{2i+1} are the encoded features of positive pairs generated from x_i, i.e., $z_{2i} = H_h(E_\theta(\tau_1(x_i)))$ and $z_{2i+1} = H_h(E_\theta(\tau_2(x_i)))$.

(b) Predictive Branch: To choose a proper predictive task, we need to consider two aspects: its ability to summarize and abstract the input, and its applicability to different datasets and tasks. In fact, many self-supervised learning tasks, such as Auto-encoder, Colorization and Inpainting, are predictive since they all aim to restore the input. But, those tasks do not have the same ability to both retain and abstract information. For example, inpainting is a stronger predictive task than autoencoding in terms of its ability to both abstract and retain information. Thus, although both of them would help in strengthening contrastive learning against feature suppression, inpainting is likely to provide more gains.

Another issue to consider is the applicability of the chosen task to various datasets. For example, colorization is applicable only to colorful RGB datasets, but not to greyscale datasets such as MNIST or medical image datasets. In contrast, a task like inpainting is easier to translate across different datasets.

Given the above considerations, we adopt inpainting as the default predictive task. In the supplemental material, we compare various tasks and show that while they all improve performance, inpainting delivers higher gains.

Figure 3 shows how PCL uses the inpainting task, where given an input image x, we first randomly mask several patches to get the masked input $M(x)$. Then the masked input is passed through an encoder network E with parameter θ, and a decoder network D, with parameter δ, to obtain the reconstruction result $D_\delta(E_\theta(M(x)))$. The prediction loss $\mathcal{L}_p$ is defined as the reconstruction error between the original input x and the reconstructed one $D_\delta(E_\theta(M(x)))$:

$$\mathcal{L}_p = ||D_\delta(E_\theta(M(x))) - x||_2.$$

(c) Training Procedure: We have empirically found that it is better to train the model in two phases. In the first phase, only the predictive branch is trained. In the second phase, both branches are trained together. In this latter case, the overall training loss is the combination of the prediction loss and the contrastive loss, i.e., $\mathcal{L} = \mathcal{L}_c + \lambda \cdot \mathcal{L}_p$. We set $\lambda = 10$ for all experiments. We also include results with different λ in the supplemental material.

(d) PCL Avoids Feature Suppression: With a combination of the prediction loss and the contrastive loss, PCL is capable of escaping the aforementioned local minimum/saddle points of infoNCE loss where only partial semantics are learned. This is because learning only part of the semantics can result in very high prediction loss. For example, if the network learns only semantics related to the background object but ignores the digit (Figure 3), all pixels related to the digit are likely to be predicted incorrectly, introducing large gradients that force the model out of the saddle point.

5. Experiments

Baselines. We use state-of-the-art contrastive learning methods as baselines, including SimCLR [4], MoCo [7], CPC [16] and BYOL [13]. The same network structure, batch size, and training epochs are used for all baselines and PCL's contrastive branch. For the contrastive branch of PCL, we apply the same training scheme as MoCo. PCL uses the predictive branch only for training. During inference it uses only the encoder, which is shared with the contrastive branch. Thus, the evaluation of PCL uses exactly the same number of parameters as the baselines.

Datasets. We experiment with the following datasets:

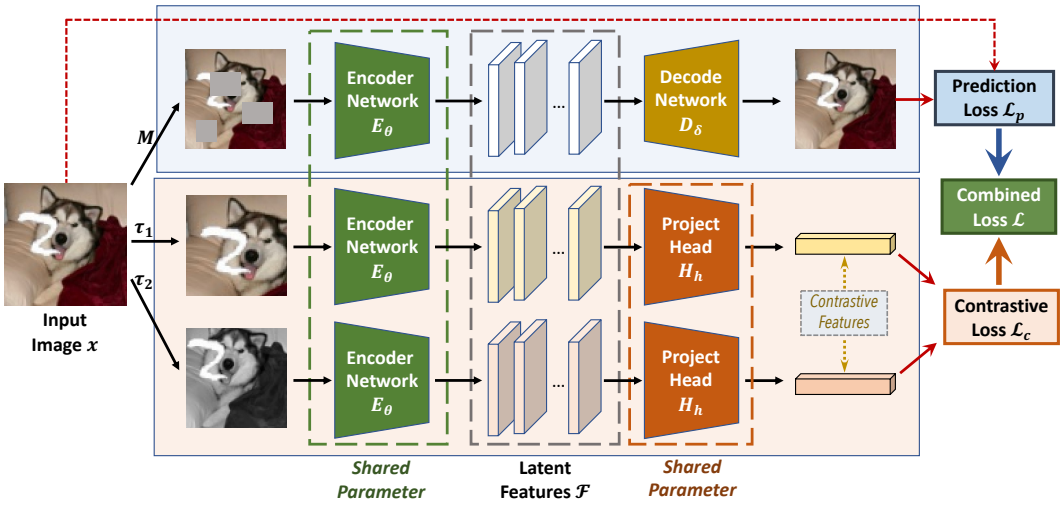


Figure 3. Illustration of the PCL framework. PCL has two branches: 1) a predictive branch, illustrated in the blue box, which ensures that the representation has enough information to restore missing patches in the input, and 2) a contrastive branch, illustrated in the orange box, which ensures that the representation keeps positive samples close to each other and away from negative samples.

- **ImageNet:** ImageNet [9] (CC BY 2.0) is a widely used image classification benchmark which contains 1.28M images in 1000 different categories. It is a standard benchmark to evaluate self-supervised learning methods [4, 7, 13].
- **MPII:** MPII [1] (the Simplified BSD License) is one of the most common datasets for the task of human pose estimation. It contains images of everyday human activities.
- **FairFace:** FairFace [20] (CC BY 4.0.) is a face attribute classification dataset, where each image contains multiple semantics including gender, age, and ethnicity.
- **Colorful-Moving-MNIST:** This is a synthetic dataset used by [27] to highlight the feature suppression problem. It is constructed by assigning each digit from MNIST a background object image selected randomly from STL-10. It supports two downstream tasks: digit and background classification.

5.1. Results

We report the main results for all datasets. The experiment setup, training details and hyper-parameter settings are provided in the supplemental material along with additional results.

ImageNet. Table 1 compares PCL with the contrastive learning baselines on the task of object classification under different data augmentations. Here, we compare PCL with SimCLR and MoCo since they use the same set of data augmentations. The results show that with fewer data augmentations, the accuracy of the contrastive learning baselines drops quickly due to feature suppression. For example, removing the color distortion augmentation significantly degrades the performance of the baseline approaches, as color distribution is known to be able to suppress other features in contrastive learning. In contrast, PCL is significantly more robust. For example, with only random cropping, PCL's Top-1 accuracy drops by only 6.9 whereas the Top-1 accuracy of SimCLR drops by 27.6 and the Top-1 accuracy of MoCo drops by 12.1. We also compare PCL with a predictive baseline [24]. For the predictive baseline, though the model is not sensitive to different augmentations, the best performance is not comparable to contrastive learning, indicating predictive learning alone is not enough to learn fine-grained representations from images.

MPII. We use PCL and the contrastive learning baselines to learn representations from MPII, and evaluate them on the task of pose estimation. Table 9 shows that PCL improves the average PCKh (the standard metric for pose estimation) over the strongest contrastive baseline by 3.7 and achieves even higher gains on important keypoints such as Head and Wrist. This is because contrastive learning is likely to focus on features irrelevant to the downstream task, such as clothes and appearances.

FairFace. Table 10 compares the contrastive learning baselines to PCL on the task of face-attribute classification. The results show how contrastive learning struggles with multi-attribute classification. Specifically, the performance of the contrastive learning baselines on ethnicity classification is close to supervised learning of that attribute (62% vs. 69%). However, their results on age and gender classifications are significantly worse than supervised learning of those attributes (44% and 78% vs. 54% and 91%). This indicates that ethnicity suppresses other features in contrastive learning. This feature is partial since there are dependencies in how ethnicity manifests itself across age and gender. In

Table 1. Performance on ImageNet with progressive removal of data augmentations for different self-supervised learning techniques. The baseline corresponds to the original set of augmentations used in SimCLR and MoCo: random flip, random resized crop, color distortion, and random Gaussian blur.

(a) ImageNet TOP-1 accuracy and its DROP w.r.t. inclusion of all augmentations.

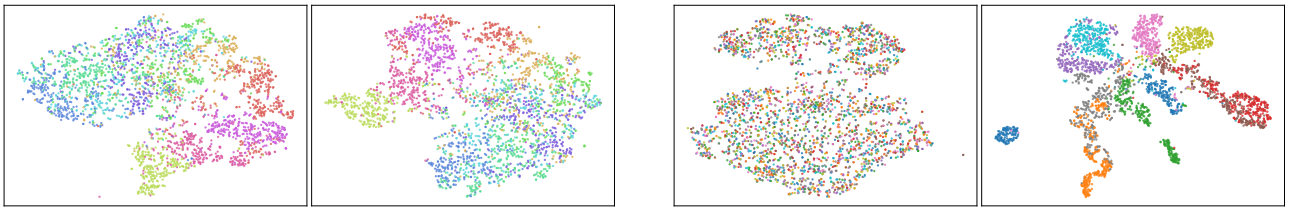
Method	Inpainting		SimCLR		MoCo		**PCL(ours)**		IMPROVE
METRIC	TOP-1	DROP	TOP-1	DROP	TOP-1	DROP	TOP-1	DROP	
Baseline	43.7	/	67.9	/	**71.1**	/	71.0	/	**-0.1**
Remove flip	43.4	-0.3	67.3	-0.6	70.6	-0.5	**70.8**	-0.2	**+0.2**
Remove blur	43.6	-0.1	65.2	-2.7	69.7	-1.4	**70.6**	-0.4	**+0.9**
Crop color only	43.2	-0.5	64.2	-3.7	69.5	-1.6	**70.1**	-0.9	**+0.6**
Remove color distort	43.5	-0.2	45.7	-22.2	60.4	-10.7	**65.9**	-5.1	**+5.5**
Crop blur only	42.8	-0.9	41.7	-26.2	59.8	-11.3	**65.1**	-5.9	**+5.3**
Crop flip only	43.3	-0.4	40.2	-27.7	59.4	-11.7	**64.6**	-6.4	**+5.2**
Crop only	42.7	-1.0	40.3	-27.6	59.0	-12.1	**64.1**	-6.9	**+5.1**

(b) ImageNet TOP-5 accuracy and its DROP w.r.t. inclusion of all augmentations.

Method	Inpainting		SimCLR		MoCo		**PCL(ours)**		IMPROVE
METRIC	TOP-5	DROP	TOP-5	DROP	TOP-5	DROP	TOP-5	DROP	
Baseline	68.3	/	88.5	/	**90.1**	/	90.0	/	**-0.1**
Remove flip	67.9	-0.4	88.2	-0.3	89.9	-0.2	**89.9**	-0.1	**+0.0**
Remove blur	68.1	-0.2	86.6	-1.9	89.7	-0.4	**89.8**	-0.2	**+0.1**
Crop color only	67.8	-0.5	86.2	-2.3	89.6	-0.5	**89.7**	-0.3	**+0.1**
Remove color distort	68.0	-0.3	70.6	-17.9	84.2	-5.9	**88.3**	-1.7	**+4.1**
Crop blur only	67.4	-0.9	66.4	-22.1	83.1	-7.0	**88.0**	-2.0	**+4.9**
Crop flip only	67.7	-0.6	64.8	-23.7	82.0	-8.1	**87.7**	-2.3	**+5.7**
Crop only	67.4	-0.9	64.8	-23.7	81.6	-8.5	**87.6**	-2.4	**+6.0**

Table 2. Performance on MPII for the downstream task of human pose estimation. ↑ indicates the larger the value, the better the performance.

METRIC		Head↑	Shoulder↑	Elbow↑	Wrist↑	Hip↑	Knee↑	Ankle↑	PCKh↑
FIXED FEATURE EXTRACTOR	SimCLR	78.4	74.6	56.7	45.2	61.8	51.3	47.1	60.8
	MoCo	79.2	75.1	57.4	45.9	62.4	52.0	47.6	61.4
	CPC	78.0	74.3	56.0	44.8	61.2	51.4	46.5	60.3
	BYOL	79.1	75.0	57.1	46.0	62.4	52.2	47.7	61.4
	PCL (ours)	**85.7**	**78.8**	**61.7**	**51.3**	**64.4**	**55.6**	**49.2**	**65.1**
	IMPROVEMENTS	**+6.5**	**+3.7**	**+4.3**	**+5.3**	**+2.0**	**+3.4**	**+1.5**	**+3.7**
FINE-TUNING	SimCLR	96.2	94.7	87.3	81.2	87.5	81.0	77.2	87.1
	MoCo	95.9	94.7	87.5	81.6	87.4	81.7	76.9	87.2
	CPC	96.0	94.5	87.0	81.1	87.3	80.8	77.0	87.0
	BYOL	96.2	94.8	87.5	81.4	87.6	81.5	77.0	87.2
	PCL (ours)	**96.3**	**94.9**	**88.1**	**82.3**	**87.9**	**82.8**	**77.8**	**87.8**
	IMPROVEMENTS	**+0.1**	**+0.1**	**+0.6**	**+0.7**	**+0.3**	**+1.1**	**+0.6**	**+0.6**
SUPERVISED		96.3	95.1	87.9	82.2	87.8	82.7	77.8	87.7



(a) SimCLR (Background) (b) PCL (Background) (c) SimCLR (Digit) (d) PCL (Digit)

Figure 4. Visualization of latent features learned using different approaches on Colorful-Moving-MNIST dataset. The color of the left two figures corresponds to background object labels, and the color of the right two figures corresponds to the digit label.

contrast, PCL is much more robust to such feature suppression problem, and its performance results on age and gender classifications are much closer to those of fully-supervised classification of those attributes.

Table 3. Performance on FairFace with different unsupervised learning methods. The models are evaluated on downstream tasks of age, gender and ethnicity classification.

Metric		Age cls Acc. (%)	Gender cls Acc. (%)	Ethn. cls Acc. (%)
Fixed feature extractor	SimCLR	43.9	78.1	61.7
	MoCo	44.5	78.6	61.9
	CPC	43.5	76.2	61.0
	BYOL	44.3	78.6	**62.3**
	PCL (ours)	**50.0**	**87.2**	61.2
	Improvement	**+5.7**	**+8.6**	**-1.1**
Fine-tuning	SimCLR	54.3	91.1	69.1
	MoCo	54.7	91.3	69.2
	CPC	54.2	91.0	68.8
	BYOL	54.6	91.5	**69.3**
	PCL (ours)	**55.3**	**92.3**	69.0
	Improvement	**+0.6**	**+0.8**	**-0.3**
Supervised on Age		55.5	78.8	45.1
Supervised on gender		43.3	92.5	45.4
Supervised on Ethn.		42.1	76.8	69.4
Supervised on All		54.8	91.9	68.8

Table 4. Performance on Colorful-Moving-MNIST under different unsupervised methods. The models are evaluated on the downstream tasks of digit classification and background object classification.

Metric		Digit cls Acc. (%)	Bkgd cls Acc. (%)
Fixed feature extractor	SimCLR	14.9	47.3
	MoCo	15.7	48.5
	CPC	15.8	35.2
	BYOL	15.5	**49.0**
	PCL (ours)	**88.3**	46.5
	Improvement	**+72.5**	**-2.5**
Fine-tuning	SimCLR	92.4	54.8
	MoCo	92.7	54.9
	CPC	92.3	54.7
	BYOL	92.7	**54.9**
	PCL (ours)	**93.3**	54.7
	Improvement	**+0.6**	**-0.2**
Supervised on digit		96.1	11.4
Supervised on bkgd		12.9	56.7
Supervised on digit & bkgd		93.0	54.5

Colorful-Moving-MNIST. We use this dataset to further investigate how contrastive learning performs on multi-attribute classification. Recall that each image in this dataset contains a digit from MNIST on a randomly selected background object from the STL-10. We investigate whether the learned representation supports both digit and background classifications. Table 11 shows that the contrastive learning baselines learn only the task of background classification, and fail to learn a representation relevant to digit classification. This shows that information related to the background prevents contrastive learning from capturing digit-relevant features. Note that the performance gap on digit classification between contrastive learning and supervised learning is very large (the accuracy is 15% vs. 93%). This is much larger than the gap we saw on FairFace because the information related to digit and background are totally independent, whereas features related to ethnicity, age, and gender have a significant overlap. In contrast, the representation learned by PCL achieves very good accuracy on both background and digit classifications.

Figure 4 provides a t-SNE visualization [29] of the learned features for SimCLR and PCL. The figure shows how predictive learning complement contrastive learning. Comparing Figures 4(c) and 4(d) reveals that PCL's predictive branch allows it to capture information about digits that is lost in SimCLR.

Finally, we run SimCLR and PCL on Colorful-Moving-MNIST with different feature dimensions of 512 and 1024, as shown in Table 5. These results show that the performance of SimCLR does not change with larger dimensions. In fact, the same result can be seen from our theoretical analysis, which proves that when increasing the feature dimensions, contrastive learning experiences many local minimums that correspond to all of the global minimums of the lower dimensions, which tend to suppress features, while PCL can escape from those local minimums.

Table 5. Performance on Colorful-Moving-MNIST with different feature dimensions under different unsupervised methods.

Method	Feature Dimension	Digit cls Acc. (%)	Bkgd cls Acc. (%)
SimCLR	512	16.0	48.4
	1024	15.8	48.6
PCL	512	88.1	46.3
	1024	88.2	46.5

6. Conclusion & Limitations

In this paper, we introduce predictive contrastive learning (PCL), a novel framework for making unsupervised contrastive learning more robust and allow it to preserve useful information in the presence of feature suppression. We theoretically analyze the reason why contrastive learning is vulnerable to feature suppression, and show that the predictive loss can help avoid feature suppression and preserve useful information. Extensive empirical results on a variety of datasets and tasks show that PCL is effective at addressing the feature suppression problem.

The problem of feature suppression is complex; and, while PCL provides an important improvement over the current SOTA, it has some limitations. First, PCL sees some performance drop with fewer augmentations. The drop however is much better than the contrastive baselines. Second,

PCL tries to abstract and preserve the information in the input, but some of this information may be unnecessary or irrelevant to the downstream tasks of interest. Yet, despite these limitations, we believe that PCL provides an important step forward toward making self-supervised learning more robust and providing richer self-supervised representations that support multi-attribute classifications and generalize well across diverse tasks.

References

[1] Mykhaylo Andriluka, Leonid Pishchulin, Peter Gehler, and Bernt Schiele. 2d human pose estimation: New benchmark and state of the art analysis. In *Proceedings of the IEEE Conference on computer Vision and Pattern Recognition*, pages 3686–3693, 2014. 2, 6, 14

[2] Philip Bachman, R Devon Hjelm, and William Buchwalter. Learning representations by maximizing mutual information across views. *arXiv preprint arXiv:1906.00910*, 2019. 1

[3] Mathilde Caron, Ishan Misra, Julien Mairal, Priya Goyal, Piotr Bojanowski, and Armand Joulin. Unsupervised learning of visual features by contrasting cluster assignments. *arXiv preprint arXiv:2006.09882*, 2020. 1

[4] Ting Chen, Simon Kornblith, Mohammad Norouzi, and Geoffrey Hinton. A simple framework for contrastive learning of visual representations. *arXiv preprint arXiv:2002.05709*, 2020. 1, 2, 5, 6, 11, 12

[5] Ting Chen, Simon Kornblith, Kevin Swersky, Mohammad Norouzi, and Geoffrey E Hinton. Big self-supervised models are strong semi-supervised learners. *Advances in Neural Information Processing Systems*, 33, 2020. 1, 2

[6] Ting Chen and Lala Li. Intriguing properties of contrastive losses. *arXiv preprint arXiv:2011.02803*, 2020. 1

[7] Xinlei Chen, Haoqi Fan, Ross Girshick, and Kaiming He. Improved baselines with momentum contrastive learning. *arXiv preprint arXiv:2003.04297*, 2020. 1, 2, 5, 6, 13

[8] Xinlei Chen and Kaiming He. Exploring simple siamese representation learning. *arXiv preprint arXiv:2011.10566*, 2020. 2

[9] Jia Deng, Wei Dong, Richard Socher, Li-Jia Li, Kai Li, and Li Fei-Fei. Imagenet: A large-scale hierarchical image database. In *2009 IEEE conference on computer vision and pattern recognition*, pages 248–255. Ieee, 2009. 6

[10] Jonas Dippel, Steffen Vogler, and Johannes Höhne. Towards fine-grained visual representations by combining contrastive learning with image reconstruction and attention-weighted pooling. *arXiv preprint arXiv:2104.04323*, 2021. 3

[11] Carl Doersch, Abhinav Gupta, and Alexei A Efros. Unsupervised visual representation learning by context prediction. In *Proceedings of the IEEE international conference on computer vision*, pages 1422–1430, 2015. 1

[12] Spyros Gidaris, Praveer Singh, and Nikos Komodakis. Unsupervised representation learning by predicting image rotations. *arXiv preprint arXiv:1803.07728*, 2018. 2

[13] Jean-Bastien Grill, Florian Strub, Florent Altché, Corentin Tallec, Pierre H Richemond, Elena Buchatskaya, Carl Doersch, Bernardo Avila Pires, Zhaohan Daniel Guo, Mohammad Gheshlaghi Azar, et al. Bootstrap your own latent: A new approach to self-supervised learning. *arXiv preprint arXiv:2006.07733*, 2020. 1, 2, 5, 6, 12, 13

[14] Tengda Han, Weidi Xie, and Andrew Zisserman. Memory-augmented dense predictive coding for video representation learning. *arXiv preprint arXiv:2008.01065*, 2020. 1

[15] Kaiming He, Haoqi Fan, Yuxin Wu, Saining Xie, and Ross Girshick. Momentum contrast for unsupervised visual representation learning. In *Proceedings of the IEEE/CVF Conference on Computer Vision and Pattern Recognition*, pages 9729–9738, 2020. 1, 2

[16] Olivier J Hénaff, Aravind Srinivas, Jeffrey De Fauw, Ali Razavi, Carl Doersch, SM Eslami, and Aaron van den Oord. Data-efficient image recognition with contrastive predictive coding. *arXiv preprint arXiv:1905.09272*, 2019. 3, 5

[17] Geoffrey E Hinton and Ruslan R Salakhutdinov. Reducing the dimensionality of data with neural networks. *science*, 313(5786):504–507, 2006. 3

[18] R Devon Hjelm, Alex Fedorov, Samuel Lavoie-Marchildon, Karan Grewal, Phil Bachman, Adam Trischler, and Yoshua Bengio. Learning deep representations by mutual information estimation and maximization. *arXiv preprint arXiv:1808.06670*, 2018. 1

[19] Dongwei Jiang, Wubo Li, Miao Cao, Ruixiong Zhang, Wei Zou, Kun Han, and Xiangang Li. Speech simclr: Combining contrastive and reconstruction objective for self-supervised speech representation learning. *arXiv preprint arXiv:2010.13991*, 2020. 3

[20] Kimmo Kärkkäinen and Jungseock Joo. Fairface: Face attribute dataset for balanced race, gender, and age. *arXiv preprint arXiv:1908.04913*, 2019. 1, 2, 6

[21] Ishan Misra and Laurens van der Maaten. Self-supervised learning of pretext-invariant representations. In *Proceedings of the IEEE/CVF Conference on Computer Vision and Pattern Recognition*, pages 6707–6717, 2020. 1

[22] Mehdi Noroozi and Paolo Favaro. Unsupervised learning of visual representations by solving jigsaw puzzles. In *European Conference on Computer Vision*, pages 69–84. Springer, 2016. 2, 11

[23] Aaron van den Oord, Yazhe Li, and Oriol Vinyals. Representation learning with contrastive predictive coding. *arXiv preprint arXiv:1807.03748*, 2018. 1, 3

[24] Deepak Pathak, Philipp Krahenbuhl, Jeff Donahue, Trevor Darrell, and Alexei A Efros. Context encoders: Feature learning by inpainting. In *Proceedings of the IEEE conference on computer vision and pattern recognition*, pages 2536–2544, 2016. 2, 6, 12

[25] Yunchen Pu, Zhe Gan, Ricardo Henao, Xin Yuan, Chunyuan Li, Andrew Stevens, and Lawrence Carin. Variational autoencoder for deep learning of images, labels and captions. *arXiv preprint arXiv:1609.08976*, 2016. 3

[26] Yonglong Tian, Dilip Krishnan, and Phillip Isola. Contrastive multiview coding. *arXiv preprint arXiv:1906.05849*, 2019. 2

[27] Yonglong Tian, Chen Sun, Ben Poole, Dilip Krishnan, Cordelia Schmid, and Phillip Isola. What makes for good views for contrastive learning. *arXiv preprint arXiv:2005.10243*, 2020. 1, 2, 6

[28] Michael Tschannen, Josip Djolonga, Paul K Rubenstein, Sylvain Gelly, and Mario Lucic. On mutual information maximization for representation learning. *arXiv preprint arXiv:1907.13625*, 2019. 1

[29] Laurens Van der Maaten and Geoffrey Hinton. Visualizing data using t-sne. *Journal of machine learning research*, 9(11), 2008. 8

[30] Pascal Vincent, Hugo Larochelle, Yoshua Bengio, and Pierre-Antoine Manzagol. Extracting and composing robust features with denoising autoencoders. In *Proceedings of the 25th international conference on Machine learning*, pages 1096–1103, 2008. 3

[31] Tongzhou Wang and Phillip Isola. Understanding contrastive representation learning through alignment and uniformity on the hypersphere. In *International Conference on Machine Learning*, pages 9929–9939. PMLR, 2020. 3

[32] Xudong Wang, Ziwei Liu, and Stella X Yu. Unsupervised feature learning by cross-level discrimination between instances and groups. *arXiv preprint arXiv:2008.03813*, 2020. 4

[33] Bin Xiao, Haiping Wu, and Yichen Wei. Simple baselines for human pose estimation and tracking. In *Proceedings of the European conference on computer vision (ECCV)*, pages 466–481, 2018. 13

[34] Mang Ye, Xu Zhang, Pong C Yuen, and Shih-Fu Chang. Unsupervised embedding learning via invariant and spreading instance feature. In *Proceedings of the IEEE Conference on computer vision and pattern recognition*, pages 6210–6219, 2019. 1

[35] Richard Zhang, Phillip Isola, and Alexei A Efros. Colorful image colorization. In *European conference on computer vision*, pages 649–666. Springer, 2016. 11, 12

[36] Chengxu Zhuang, Alex Lin Zhai, and Daniel Yamins. Local aggregation for unsupervised learning of visual embeddings. In *Proceedings of the IEEE/CVF International Conference on Computer Vision*, pages 6002–6012, 2019. 1

Appendix A: Additional Results

In this section, we provide additional results to better understand PCL.

Table 6. Comparison of different predictive tasks for PCL's predictive branch. The table shows the performance of PCL on Colorful-Moving-MNIST with different predictive tasks in its predictive branch for the fixed feature encoder setting. Colorization achieves good performance on background classification, but bad performance on digit classification since the MNIST digits have no RGB information. Inpainting achieves the best performance among these predictive tasks.

	Colorful-Moving-MNIST	
Recon. Tasks	DIGIT CLS ACC. (%)	BKGD CLS ACC. (%)
No Recon.	15.7	**48.5**
Jigsaw Puzzle	16.1	47.7
Colorization	63.9	47.0
Autoencoder	65.6	42.9
Inpainting	**88.3**	46.5

Comparison of Different Predictive Tasks for PCL's Predictive Branch: In PCL, we choose the inpainting task for the predictive branch. However, other predictive tasks can be potentially used for the predictive branch. In this section, we evaluate the performance of PCL with different predictive tasks including Jigsaw Puzzle [22], inpainting, auto-encoder and colorization [35]. Table 6 shows PCL's performance using different predictive task on Colorful-Moving-MNIST under the fixed feature extractor setting. As shown in the table, all predictive tasks except for Jigsaw Puzzle significantly reduce errors on digit classification in comparison to using contrastive learning without any predictive task. This is because the Jigsaw Puzzle task does not require the features to be able to reconstruct the original image, but just to restore the order of different patches. Learning the background object is sufficient to solve Jigsaw, and the network does not have incentives to learn the digit. The table also shows that inpaintaing compares favorably to other predictive tasks and achieves good performance on both downstream tasks. Hence, we use inpainting as the default predictive task in PCL.

Masking as a Data Augmentation vs. PCL: In the predictive branch, PCL introduces masked input images. Some may wonder whether the improvements are coming from this masking operation, since cutting out the input signals can be viewed as one way of augmentation [4]. However, here in Table 7, we show the performance of MoCo with and without masking augmentation on Colorful-Moving-MNIST (we use the same masking strategy as the predictive branch of PCL). As shown in the table, the performance of MoCo stays similar with or without masking augmentation. This demonstrate that the improvements of PCL do not come from this augmentation.

Table 7. Performance of MoCo on Colorful-Moving-MNIST without masking augmentation (fixed feature encoder setting). The results demonstrate that simply adding masking as a data augmentation does not achieve similar improvements as PCL.

	Colorful-Moving-MNIST	
Recon. Tasks	DIGIT CLS ACC. (%)	BKGD CLS ACC. (%)
MoCo w/o masking	15.7	**48.5**
MoCo w/ masking	15.2	48.4
PCL	**88.3**	46.5

Warm-up Training: To show the effectiveness of the proposed warm-up training strategy (Sec. 3 (c)), we compare the results of warm-up training with the results of directly using the combined loss $\mathcal{L}$ (i.e., combining the prediction loss and the contrastive loss) from the beginning. As shown in Table 12, without the warm-up training, on Colorful-Moving-MNIST, PCL largely degenerates to become similar to the contrastive learning baselines and cannot learn good features related to digit classification. This indicates that without the warm-up phase, the contrastive loss can dominate the network causing it to suppress feature at the beginning, and that the network cannot later jump out of the local minimum that suppress feature. On the other hand, with warm-up training, the network first learns a coarse representation; then the contrastive loss helps the network learn more fine-grained representations.

Performance of PCL with different λ: In PCL, the combined loss is a weighted average of the prediction loss and the contrastive loss, i.e., $\mathcal{L} = \mathcal{L}_c + \lambda \cdot \mathcal{L}_p$. In the experiments of main paper, λ is set to 10. In this section, we investigate how different λ affects the performance of PCL. Note that when $\lambda = 0$, PCL degenerates to contrastive learning; when $\lambda \to \infty$, PCL degenerates to predictive learning.

Table 8 compares the performance of PCL with different λ. As we can see from the results, when $\lambda < 100$, with larger λ, the accuracy of the digit classification increases, while the accuracy of background classification decreases. Moreover, the λ values between 10 and 100 gives quite similar performances, indicating a balancing between contrastive loss and prediction loss. For $\lambda > 100$, the prediction loss dominates the contrastive loss and harm the performance. Therefore, we fix $\lambda = 10$ for all experiments.

Predictive Learning vs. PCL: In the main paper, we mainly compare PCL with contrastive learning since contrastive learning is the current unsupervised learning SOTA on ImageNet and outperforms predictive learning by a large

Table 8. Digit classification and background classification accuracy of PCL with different λ on Colorful-Moving-MNIST dataset.

λ	0	1	5	10	25	50	100	200	500	1000
DIGIT ACC (%)	15.7	48.6	69.8	88.3	88.2	88.3	88.1	87.5	86.3	85.0
BKGD ACC (%)	48.5	47.9	47.5	47.2	47.2	47.1	47.0	45.7	44.5	40.5

Table 9. Performance of PCL and predictive baselines on MPII for the downstream task of human pose estimation. ↑ indicates the larger the value, the better the performance.

METRIC		Head↑	Shoulder↑	Elbow↑	Wrist↑	Hip↑	Knee↑	Ankle↑	PCKh↑
FIXED FEATURE EXTRACTOR	Inpainting	83.4	75.2	53.6	44.4	56.4	44.3	45.7	59.0
	Colorization	79.5	71.2	49.6	42.1	54.2	40.7	41.9	55.1
	Autoencoder	79.1	70.1	47.2	41.6	51.9	39.1	40.3	53.8
	PCL (ours)	**85.7**	**78.8**	**61.7**	**51.3**	**64.4**	**55.6**	**49.2**	**65.1**
	IMPROVEMENTS	**+2.3**	**+3.6**	**+8.1**	**+6.9**	**+8.0**	**+11.3**	**+3.5**	**+6.1**
FINE-TUNING	Inpainting	96.3	**95.2**	87.9	82.1	87.8	82.5	77.6	87.7
	Colorization	96.2	95.1	87.7	82.1	87.8	82.5	77.5	87.6
	Autoencoder	96.0	94.9	87.6	82.0	87.6	82.4	77.3	87.5
	PCL (ours)	**96.3**	94.9	**88.1**	**82.3**	**87.9**	**82.8**	**77.8**	**87.8**
	IMPROVEMENTS	**+0.0**	**-0.3**	**+0.2**	**+0.2**	**+0.1**	**+0.3**	**+0.2**	**+0.1**

Table 10. Performance on FairFace with PCL and different predictive unsupervised learning methods. The models are evaluated on downstream tasks of age, gender and ethnicity classification.

METRIC		AGE CLS ACC. (%)	GENDER CLS ACC. (%)	ETHN. CLS ACC. (%)
FIXED FEATURE EXTRACTOR	Inpainting	46.3	83.6	52.9
	Colorization	46.1	82.9	53.8
	Autoencoder	44.3	80.1	50.7
	PCL (ours)	**50.0**	**87.2**	**61.2**
	IMPROVEMENT	**+3.7**	**+3.6**	**+7.4**
FINE-TUNING	Inpainting	55.0	91.8	68.3
	Colorization	54.9	92.0	68.6
	Autoencoder	54.5	91.3	67.9
	PCL (ours)	**55.3**	**92.3**	**69.0**
	IMPROVEMENT	**+0.3**	**+0.3**	**+0.4**

Table 11. Performance on Colorful-Moving-MNIST under different methods. The models are evaluated on the downstream tasks of digit classification and background object classification.

METRIC		DIGIT CLS ACC. (%)	BKGD CLS ACC. (%)
FIXED FEATURE EXTRACTOR	Inpainting	84.7	35.0
	Colorization	80.7	38.4
	Autoencoder	81.0	32.9
	PCL (ours)	**88.3**	**46.5**
	IMPROVEMENT	**+3.2**	**+8.1**
FINE-TUNING	Inpainting	92.9	54.5
	Colorization	92.5	54.5
	Autoencoder	92.4	54.1
	PCL (ours)	**93.3**	**54.7**
	IMPROVEMENT	**+0.4**	**+0.2**

Table 12. Performance of PCL on Colorful-Moving-MNIST with and without warm-up training.

	Colorful-Moving-MNIST	
Warm-up Training	DIGIT CLS ACC. (%)	BKGD CLS ACC. (%)
No	24.9	**47.8**
Yes	**88.3**	46.5

margin [4, 13]. Here, we also compare PCL with predictive learning, such as inpainting, colorization and autoencoder, on various datasets to demonstrate the effectiveness of the contrastive branch of PCL. Tables [4-6] compare PCL with Inpainting [24], Colorization [35] and Auto-encoder on the RGB datasets. The results demonstrate that PCL outperforms all predictive learning baselines by a large margin. This is because the contrastive branch in PCL can significantly improve the quality of the learned representation so it can achieve much better performance on downstream tasks.

Appendix B: Additional Proofs

Here we formally prove Corollary 1 and 2.

Corollary 3. *For any lifting operator $\mathcal{T}_\sigma$, if $\hat{Z} = \{\hat{z}_i\}$ is a stationary point of $\mathcal{E}_{\texttt{limNCE}}(Z; X, \tau, d_1)$, then $\mathcal{T}_\sigma(\hat{Z})$ is a*

stationary point of $\mathcal{E}_{\texttt{limNCE}}(Z; X, \tau, d_2)$.

Proof. The proof is in the supplemental material. □

Proof. $\hat{Z}$ is a stationary point of $\mathcal{E}_{\texttt{limNCE}}(Z; X, \tau, d_1)$ implies $\nabla_{z_i}\mathcal{E}_{\texttt{limNCE}}(\hat{Z}; X, \tau, d_1) = 0$. Therefore, by Lemma 2, $\nabla_{\hat{z}_i}\mathcal{E}_{\texttt{limNCE}}(\mathcal{T}_\sigma(\hat{Z}); X, \tau, d_2) = \mathcal{T}_\sigma\left(\nabla_{z_i}\mathcal{E}_{\texttt{limNCE}}(\hat{Z}; X, \tau, d_1)\right) = 0$. □

Corollary 4. *For any lifting operator* $\mathcal{T}_\sigma$*, if* $\hat{Z} = \{\hat{z}_i\}$ *is a global minimum of* $\mathcal{E}_{\texttt{limNCE}}(Z; X, \tau, d_1)$ *with a positive definite Hessian matrix, then* $\mathcal{T}_\sigma(\hat{Z})$ *is a saddle point or a local minimum of* $\mathcal{E}_{\texttt{limNCE}}(Z; X, \tau, d_2)$.

Proof. From Corollary 3, $\mathcal{T}_\sigma(\hat{Z})$ is a stationary point of $\mathcal{E}_{\texttt{limNCE}}(Z; X, \tau, d_2)$. Since the Hessian matrix of $\mathcal{E}_{\texttt{limNCE}}(Z; X, \tau, d_1)$ at $\hat{Z}$ is positive definite, $\forall r > 0, \exists Z' \in B_r(\hat{Z})$ s.t. $\mathcal{E}_{\texttt{limNCE}}(Z'; X, \tau, d_1) > \mathcal{E}_{\texttt{limNCE}}(Z; X, \tau, d_2)$, where $B_r(Z) = \{Z' \in \mathbb{S}^{d-1} | \, ||Z - Z'||_2 < r\}$ is the neighborhood of Z with radius r. Therefore, $\mathcal{E}_{\texttt{limNCE}}(\mathcal{T}_\sigma(Z'); X, \tau, d_1) > \mathcal{E}_{\texttt{limNCE}}(\mathcal{T}_\sigma(Z); X, \tau, d_2)$ (Lemma 1). Note that $Z' \in B_r(\hat{Z}) \rightarrow \mathcal{T}_\sigma(Z') \in B_r(\mathcal{T}_\sigma(\hat{Z}))$. Therefore, $\forall r > 0, \exists \mathcal{T}_\sigma(Z') \in B_r(\mathcal{T}_\sigma(\hat{Z}))$ s.t. $\mathcal{E}_{\texttt{limNCE}}(\mathcal{T}_\sigma(Z'); X, \tau, d_1) > \mathcal{E}_{\texttt{limNCE}}(\mathcal{T}_\sigma(Z); X, \tau, d_2)$. Therefore, $\mathcal{T}_\sigma(\hat{Z})$ is not a local maximum, so it can only be a local minimum or a saddle point of $\mathcal{E}_{\texttt{limNCE}}(Z; X, \tau, d_2)$. □

Appendix C: Implementation Details

In this section, we provide the implementation details of the models used in our experiments. All experiments are performed on 8 NVIDIA Titan X Pascal GPUs. On ImageNet, training takes ∼100 hours. On each dataset, we fix the batch size and training epochs for different baselines for a fair comparison. Other parameters for each baseline follow the original paper to optimize for its best performance. Code will also be released upon acceptance of the paper.

ImageNet: We use a standard ResNet-50 for the encoder network. The decoder network is a 11-layer deconvolutional network. The projection head for contrastive learning is a 2-layer non-linear head which embeds the feature into a 128-dimensional unit sphere. The same network structure is used for all baselines and PCL.

We follow the open repo of [7] for the implementation of MoCo baselines and PCL on ImageNet. For results on SimCLR, we follow the results reported in [13]. All baselines and PCL is trained for 800 epochs with a batch size of 256. For the predictive branch of PCL and the predictive baseline, we mask out 3 to 5 rectangles at random locations in the image. The size of each square is chosen by setting its side randomly between 40 and 80 pixels. For the contrastive branch of PCL, we apply the same training scheme as MoCo. The first 10 epochs are warm-up epochs, where we only train the network with the prediction loss $\mathcal{L}_p$. For later training, we set $\lambda = 10$. For other RGB datasets, we mainly follows similar implementation as ImageNet.

MPII: We use the network structure similar to the one in [33]. We use a ResNet-50 for the encoder network. Three deconvolutional layers with kernel size 4 and one convolutional layer with kernel size 1 is added on top of the encoded feature to transfer the feature into 13 heatmaps corresponding to 13 keypoints. For the contrastive branch, a 2-layer non-linear projection head is added on top of the encoded feature and embeds the feature into a 128-dimensional unit sphere. For the predictive branch, a decoder network similar to the pose estimation deconvolution network (only the number of output channels is changed to 3) is used to reconstruct the original image. Other implementation details are the same as ImageNet.

For the baselines and PCL, we train the network for 300 epochs with a batch size of 256. The data augmentation is the same as the baseline augmentations on ImageNet. For PCL, the first 10 epochs are warm-up epochs, where we only train the network with the prediction loss $\mathcal{L}_p$.

FairFace: We use a standard ResNet-50 for the encoder network. The decoder network is a 11-layer deconvolutional network. The projection head for contrastive learning is a 2-layer non-linear head which embeds the feature into a 128-dimensional unit sphere. The same network structure is used for all baselines and PCL.

For the baselines and PCL, we train the network for 1000 epochs with a batch size of 256. The data augmentation is the same as the baseline augmentations on ImageNet. For PCL, the first 30 epochs are warm-up epochs, where we only train the network with the prediction loss $\mathcal{L}_p$.

Colorful-Moving-MNIST: We use a 6-layer ConvNet for the encoder. The encoder weights for the predictive and contrastive branches are shared. The decoder is a 6-layer deconvolutional network symmetric to the encoder. The projection head for contrastive learning is a 2-layer non-linear head which embeds the feature into a 64-dim normalized space.

We use the SGD optimizer with 0.1 learning rate, 1e-4 weight decay, and 0.9 momentum to train the model for 200 epochs. The learning rate is scaled with a factor of 0.1 at epoch 150 and 175. The batch size is set to 512. The temperature for contrastive loss is set to 0.1. For PCL, the first 30 epochs are warm-up epochs, where we only train the network with the prediction loss $\mathcal{L}_p$.

For PCL, for each input image after augmentation with a size of 64 by 64 pixels, we randomly mask out 3 to 5 rectangle patches at random locations in the image and fill them with the average pixel value of the dataset. The size of each square is chosen by setting its side randomly between 10 and 16 pixels.

Appendix D: Experiments' Setup and Evaluation Metrics

Setup. On ImageNet, as common in the literature, we evaluate the representations with the encoder fixed and only the linear classifier is trained. On all other datasets, we evaluate the representations under two different settings: fixed feature encoder setting and fine-tuning setting. In the fixed feature encoder setting, the ResNet encoder is fixed and only the classifier (FairFace, Colorful-Moving-MNIST) or the 4-layer decoder network (MPII); In the fine-tuning setting, the encoder is initialized with the pre-trained model and fine-tuned during training.

Evaluation Metrics. For ImageNet, FairFace and Colorful-Moving-MNIST, the evaluation metrics are the standard Top-1 classification accuracy. For MPII, we evaluate the learned representations under the single pose estimation setting [1]. Each person is cropped using the approximate location and scale provided by the dataset. Similar to prior works, we report the PCKh (Percentage of Correct Keypoints that uses the matching threshold as 50% of the head segment length) value of each keypoint and an overall weighted averaged PCKh over all keypoints (head, shoulder, elbow, wrist, hip, knee, ankle).